JOURNAL OF Materials CHEMISTRY
Feature Article

Ferroelectric ceramics: defects and dielectric relaxations

C. Elissalde and J. Ravez

ICMCB-CNRS, 87 Avenue du Docteur, A.Schweitzer 33608 Pessac cedex, France

Received 19th December 2000, Accepted 26th April 2001
First published as an Advance Article on the web 14th June 2001

Dielectric relaxations in ferroelectric ceramics occur at various frequencies, depending on the type of chemical or physical defects. These defects depend on either intrinsic or extrinsic heterogeneities due to special heat treatments (quenching, annealing,…), ionic substitutions, grain size additives, and grain boundary nature. The value of the relaxation frequency f_r increases from about 10^2 to 10^{12} Hz as the scale of the defect phenomenon decreases from microstructure, to nanostructure, to unit-cell, to atomic vibrations. This type of study requires a pluridisciplinary approach involving solid state chemistry, materials science, solid state physics and various industrial aspects. The applications in the area of electronic ceramics are related to the value of f_r. In absorbants, the usable frequency is close to f_r, whereas it is far from f_r in good insulators. In view of numerous experimental examples, a classification is proposed to predict which materials may be suitable for a given application.

1. Introduction

Ferroelectricity is characterized crystallographically by a shift of atoms from their positions in the paraelectric phase. The gravity centres of the positive and negative charges do not coincide when $T<T_C$ (Curie temperature). A spontaneous polarization, $\vec{P}_s$, is thus created in the crystal even without the application of an external field. The orientation of $\vec{P}_s$ along the polar axis can be reversed by an applied electric field. In addition, ferroelectrics are characterized by a maximum of the real part, ε', of the complex permittivity at the Curie temperature T_C. Above T_C, the material becomes paraelectric.

An ideal ferroelectric should be a good electrical insulator, as it keeps its spontaneous polarization, *i.e.* its electric charge. In fact, such a property depends on external stresses such as the temperature and the applied electric field frequency. A simple example related to all ferroelectric types concerns the depolarization current resulting from a temperature increase, which is responsible for pyroelectric properties; a peak in the pyroelectric coefficient p ($p=\delta P_s/\delta T$) is obtained just below T_C. This effect is purely ferroelectric and is related to the decrease in $\vec{P}_s$ with temperature and its cancellation at T_C.

There is a more complex reason for the decrease in insulating properties. When an alternating current is applied to a sample, the dipoles responsible for the polarization are no longer able to follow the oscillations of the electric field at certain frequencies. The field reversal and the dipole reorientation become out-of-phase, giving rise to an energy dissipation. Such an effect is called dielectric relaxation and may be evidenced by a drop in ε' and a maximum in the imaginary part of the permittivity, ε'', at the relaxation frequency f_r (see definitions of ε' and ε'' in next section). The value of f_r may range from low to high frequencies depending on the type of chemical or physical defects related to the dipoles considered. Defects may cause modifications of the short and/or long-range interactions in inorganic ferroelectrics. More generally, ferroelectric behaviour and dielectric properties are very sensitive to both external (temperature, electric field, ionic substitution,…) and intrinsic (defect, domain configuration,…) modifications because the polarization is largely affected.

This review is made up of three main parts:

(1) Firstly, some basic definitions are given. In particular, dielectric terms are defined. A schematic diagram illustrating the various relaxation and resonance types in the frequency spectrum is proposed. Mechanisms of polarization are described. The models used to illustrate the dielectric relaxation are presented.

(2) Methods for dielectric measurements are presented in a second part. The dielectric spectroscopy requires different methods of measurement according to the frequency range; they are briefly described.

(3) Finally, an overview of the different types of relaxation is given. In each case, examples which evidence relations between relaxation phenomena and defect aspects are given. The different interpretations found in the literature for the collected results are presented.

The aim of the present work is to list the main types of dielectric relaxations encountered in ferroelectric materials and to study how the value of f_r is related to the scale of the defect phenomenon. In view of such correlations, the ultimate purpose is to establish a classification in order to predict the most suitable material for a given application. Only octahedral-type ferroelectrics are taken into consideration.

The science of dielectrics is multidisciplinary encompassing the fields of physics, chemistry and electrical engineering. The present article is essentially destined to help chemists who prepare and characterize new ferroelectric materials to interpret the temperature and frequency dependences of the permittivities.

2. Definitions

In ferroelectrics, a dielectric relaxation phenomenon reflects the delay (time dependence) in the frequency response of a group of dipoles submitted to an external applied field. Because the polarization vector cannot always follow the variation of the alternating field, the frequency response is expressed in terms of the complex dielectric permittivity ε^*:

$$\varepsilon^*(\omega)=\varepsilon'(\omega)-i\varepsilon''(\omega) \quad (1)$$

where $\omega=2\pi f$ is the angular frequency; f is the circular frequency (in hertz) of the oscillating field and i a complex number ($i^2=-1$). The real (ε'; component in phase with the field) and imaginary (ε''; component in quadrature) parts of the permittivity are dependent on each other as shown by the

DOI: 10.1039/b010117f

Kramers–Kronig relations:

$$\varepsilon'(\omega)-\varepsilon_\infty=2/\pi\int_0^\infty \varepsilon''(\omega')\frac{\omega'}{(\omega')^2-\omega^2}\mathrm{d}\omega' \quad (2)$$

$$\varepsilon''(\omega)=2/\pi\int_0^\infty (\varepsilon'(\omega')-\varepsilon_\infty)\frac{\omega}{(\omega')^2-\omega^2}\mathrm{d}\omega' \quad (3)$$

where ω' is an integration variable and ε_∞ is the high frequency dielectric constant.

Such relations evidence the correlation between dispersion (variation of ε' as a function of frequency) and absorption (non-zero value of ε''): any dielectric dispersion is accompanied by an absorption peak. ε' is correlated with the polarization of the system; ε'' with the energy losses.

Over a wide frequency range, different types of polarization cause several dispersion regions (Fig. 1). The critical frequency, characteristic of each contributing mechanism, depends on the nature of the dipoles. When the frequency increases, the number of mechanisms involved in the dynamic polarization decreases. At very high frequencies, only the electronic contribution of the polarization remains. A decrease of ε' is observed with decreasing frequency. Each polarization mechanism is characterized by a critical frequency f_r (relaxation frequency) corresponding to the maximal phase shift between the polarization P and the applied electric field E; a maximum of dielectric losses ($\tan\delta=\varepsilon''/\varepsilon'$ is the loss factor) occurs. The orientation polarizations, *i.e.* interfacial polarization (space charges) and dipole polarization, are observed from low to microwave frequencies. The force opposed to the motion is here of a frictional nature and the resulting dynamics are thus of the relaxational type. The deformation polarizations, *i.e.* ionic (oscillations of ions) and electronic polarizations (displacement of electrons with respect to the nuclei), are detected in short microwave and infrared ranges. The latter mechanisms lead to resonance-type dielectric dispersions (vibrational process, harmonic oscillator type).

The concept of dipoles giving rise to polarization was introduced by Debye. The Debye model considers the reorientation of non-interacting dipoles in a purely viscous environment without an elastic restoring force. The expression for the complex permittivity is:

$$\varepsilon^*(\omega)=\varepsilon_\infty+\frac{\varepsilon_s-\varepsilon_\infty}{1+i\omega\tau} \quad (4)$$

Separation of the real and imaginary parts of the permittivity gives:

$$\varepsilon'=\varepsilon_\infty+\frac{\varepsilon_s-\varepsilon_\infty}{1+(\omega\tau)^2} \quad (5)$$

$$\varepsilon''=\frac{\varepsilon_s-\varepsilon_\infty}{1+(\omega\tau)^2}\omega\tau \quad (6)$$

where τ is the relaxation time, ε_s is the permittivity at low frequency ($f\ll$relaxation frequency) and ε_∞ the one at high frequency ($f\gg$relaxation frequency). ε' decreases to ε_∞ with increasing frequency and ε'' is maximal at the frequency $\omega=1/\tau$ (Fig. 2).

In the case of dipoles correlated through ferroelectric-type interactions, it is possible to translate the thermal variation of permittivity at various frequencies (suitable to characterize the transition and given classically) into frequency dielectric dispersion curves at fixed temperatures. Argand diagrams (ε'' *versus* ε') are also sometimes used for relaxation studies instead of the temperature and frequency variations of ε' and ε''. The corresponding curves are of course related to each other (Fig. 2). The obtained curve is a semi-circle centered on the abscissa axis at the $(\varepsilon_s-\varepsilon_\infty)/2$ point. Two parameters are characteristic of the Debye relaxation: the relaxation step $\Delta\varepsilon'=\varepsilon_s-\varepsilon_\infty$ and the relaxation time τ. The dielectric dispersion $\Delta\varepsilon'$ is then obtained by extrapolating at very low frequency ($f\ll f_r$) for ε_s and at infinite frequency ($f\gg f_r$) for ε_∞. Such parameters are related to the dipole characteristics: $\Delta\varepsilon'$ is related to both the microscopic dipolar moment p and the number N of relaxing dipoles through the Langevin relation:

$$\varepsilon_s-\varepsilon_\infty\approx Np^2/3kT \quad (7)$$

k is the Boltzmann constant ($k=8.617385$ eV K^{-1}).

The value of τ is correlated with the energy barrier ΔE separating the two minima corresponding to the two equivalent positions of the non-interacting dipoles in a double-well

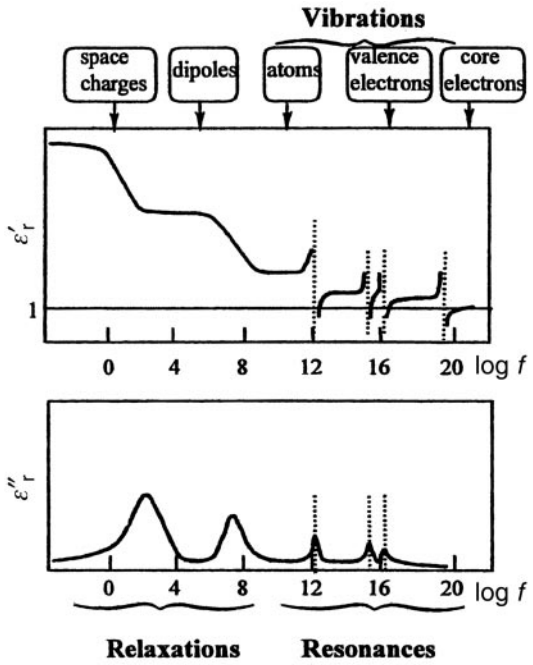

Fig. 1 Schematic representation of various relaxation and resonance types, *f*/Hz.

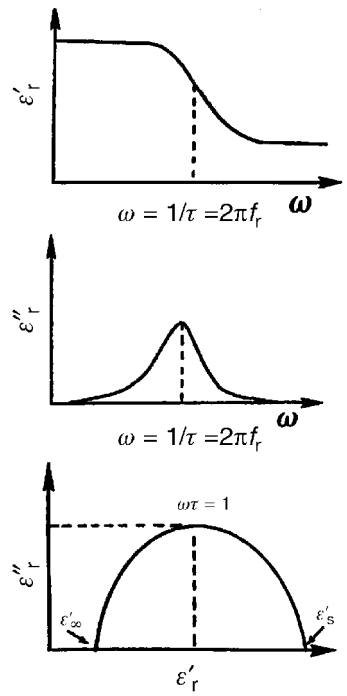

Fig. 2 Frequency dependences of ε'_r and ε''_r and an Argand diagram: Debye model.

potential (viscous interaction between the dipole and the environment). The variation of the relaxation time may be expressed as a thermally activated process:

$$\tau = \tau_0 \exp(\Delta E/kT) \quad (8)$$

with $\tau_0 = 1/\omega_0$, ω_0 being an extrapolated attempt frequency. The atoms are oscillating through the equilibrium position at the frequency $\omega_0/2\pi$ and acquire sufficient energy to cross the barrier.

In polar dielectrics, corrections to the simple Debye model are often necessary. Cole–Cole plots (Argand diagram, *i.e.* ε'' *versus* ε') reflect the deviation from the ideal Debye model and introduce a parameter α which reflects a distribution of the relaxation time.[1]

$$\varepsilon^*(\omega) = \varepsilon_\infty + \frac{\varepsilon_s - \varepsilon_\infty}{1 + (j\omega\tau)^\alpha} \quad (9)$$

Another example is the presence of conductivity, σ, which leads to an additional term in the Debye equation:

$$\varepsilon^*(\omega) = \varepsilon_\infty + \frac{\varepsilon_s - \varepsilon_\infty}{1 + (j\omega\tau)^\alpha} - j\frac{\sigma}{\omega} \quad (10)$$

(j is a complex number).

In this latter case, the complex impedance is usually measured. Charge carriers in dielectric materials have to be considered in polarization mechanisms.[2,3] The electric field can interact in a solid not only through reorientation of the electric dipoles but also through the displacement of the charge carriers. The key point is the degree of localization of these carriers. Mobile or free charges (electrons or holes) lead to a significant contribution only up to 10^{11} Hz. On the contrary, bound charges can be considered as dipoles and participate in polarization. A dissipation can arise from the hopping process in ionic conductivity. The hopping ionic motion through defects is a thermally activated process and its contribution is observed at high temperature. A carrier leading to a local lattice deformation and trapped in the potential well, *i.e.* a polaron, contributes to the dielectric properties particularly at very low temperature. Space charges (carriers located at the grain boundary in polycrystalline materials) act as dipoles under an ac field and participate in polarization; the corresponding materials are called grain boundary layer dielectrics. All these contributions lie in the frequency range 10 Hz–1 MHz according to the temperature which is a determining parameter in conduction phenomena.

The classical model of Debye allows for characterization of the impedance behaviour. The material is then described electrically by a parallel equivalent circuit of pure resistance R and capacitance C. The impedance of this model is $Z^* = R/(1 + i\omega/\omega_1)$, where ω_1 is the characteristic frequency of the circuit, $\omega_1 = 1/RC$. The response in the Z^* plane for a single parallel RC element is a semi-circle which passes through the origin and gives a low frequency intersection on the real axis corresponding to the resistance of the element. Note that in a polycrystalline sample, the equivalent circuit is formed by parallel RC circuits in series. In this way grain and grain boundary contributions are taken into account. As complex permittivity and complex impedance are related through $Z^* = 1/Y^* = 1/(i\omega C_0 \varepsilon^*)$, a relaxation in Z space (Fig. 3) can be transformed into a permittivity frequency spectrum. Real and imaginary parts of ε^* can be affected by the conduction, especially in the low frequency range. An increase in both ε'_r and ε''_r is observed when the frequency decreases. No loss peak appears when the ionic conductivity dominates the dielectric response. Experimental data can also be analyzed in complex modulus formalism, $M^* = 1/\varepsilon^* = j(\omega C_0)Z^*$, which allows a reduction of the grain boundary contribution. The relaxation frequency can be determined by plotting M''/M''_{max} as a function of frequency (M'' is the imaginary part of the complex modulus; M''_{max} is the maximum value). Impedance spectroscopy is particularly suitable for reflecting microstructural features in ceramics since it allows the separation of bulk and grain boundary contributions.

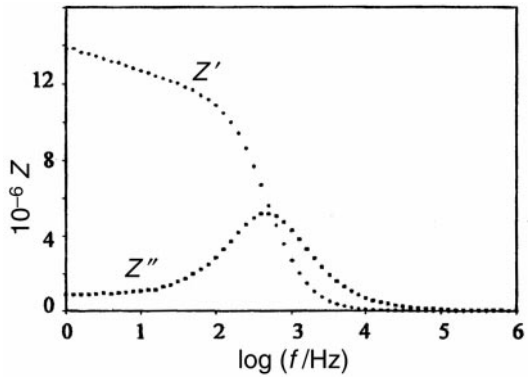

Fig. 3 Frequency dependences of Z' and Z''.

3. Dielectric characterization

The main dielectric function generally used to describe the dielectric dispersion is the complex permittivity. Usually the representation of the data is the variation of ε'_r, ε''_r and tan δ as a function of temperature and *versus* frequency. ε'_r is the relative real part of the permittivity $\varepsilon'_r = \varepsilon'/\varepsilon_0$ with the vacuum permittivity $\varepsilon_0 = 8.84 \times 10^{-12}$ C V^{-1} m^{-1}. As seen in the previous section, various kinds of dipoles and phonon modes cause several dispersion regions. The investigation of the dielectric constants over a wide frequency range, *i.e.* dielectric spectrum, is necessary to study relaxations. The dielectric spectroscopy requires different methods of measurement according to the frequency range.

From a few Hz to the lower MHz region, an impedance bridge is frequently used. ε'_r and ε''_r values are deduced from the capacitance, C, and the loss factor tan δ:

$$\varepsilon'_r = C(\varepsilon_0 S/e) \qquad \varepsilon''_r = \varepsilon'_r \times \tan\delta$$

where ε_0 is the permittivity of vacuum, S the electrode surfaces and e the sample thickness. Moreover an impedance analyzer allows measurement of the complex impedance (Z^*) of an electric circuit as a function of frequency. ε'_r and ε''_r are deduced from the real and imaginary parts of the complex admittance ($Y^* = 1/Z^*$). In the meter and decimeter wave range (3 MHz–3 GHz), network analyzers are used. Methods involving a coaxial line are considered for studies as a function of frequency. In the centimeter and millimeter wave region (30–200 GHz) measurements are performed in cavities, wave guides (reflection and transmission measurements) or free space methods.

4. Overview of the various dielectric relaxations

4.1. Low frequency relaxations

Space charge relaxations. A primary example concerns $Ba_{1-x}Pb_xTiO_3$ perovskite ceramics.[4,5] The ferroelectric Curie temperature T_C increases with x, *i.e.* with lead content. Fig. 4 shows that in addition to the ε'_r peak at T_C, a second diffuse anomaly occurs for $T > T_C$ at $T(\varepsilon'_{r\,max})$. When the frequency increases, the value of $T(\varepsilon'_{r\,max})$ also increases while ε'_r decreases. In addition, the value of ε''_r increases very strongly with temperature. This dielectric dispersion is related to a conductivity phenomenon which obeys an Arrhenius type thermal activation law. The value of the relaxation frequency f_r increases with T. In fact, when such ceramics were sintered, weight losses were caused by loss of volatile PbO. New

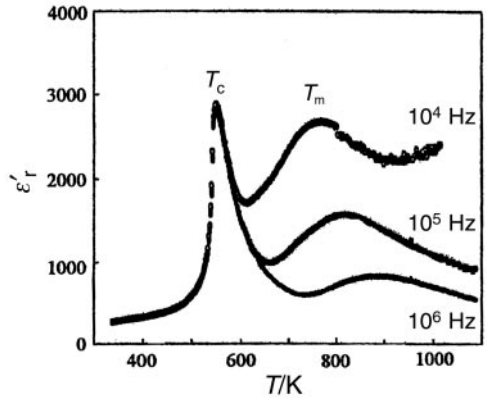

Fig. 4 Temperature dependence of ε'_r at three frequencies (10^4, 10^5 and 10^6 Hz) for a ceramic with composition $Ba_{0.7}Pb_{0.3}TiO_3$.[4]

ceramics were prepared by lower temperature sintering of powders obtained by a coprecipitation method. The temperature dependence of ε'_r then showed the disappearance of the diffuse anomaly above T_C (Fig. 5). The relaxation was thus related to the volatility of PbO. In fact, the conductivity was of anionic type due to oxygen defects in the perovskite crystalline network.

Yellow ceramics of TKWB type and $Ba_3(Nb_4Ti)O_{15}$ composition constitute a similar example.[6] For materials sintered at 1573 K in an air atmosphere, there is a maximum of ε'_r at $T_C = 450$ K and a very strong frequency dielectric dispersion leading to another maximum for $T > T_C$, at about $T_m = 500$ K, at low frequency. Such ceramics annealed at 1073 K under 1000 bar of oxygen pressure for 48 h lead to the quasi disappearance of the frequency dispersion for $T > T_C$. Complex impedance measurements have shown the mechanism responsible for this dielectric relaxation to be related to an electronic–anionic mixed conduction.[7]

Concerning ceramics of the TKWB type and $Sr_3(Nb_4Ti)O_{15}$ composition, the dielectric relaxation occurs at low temperatures close to 150 K and partially masks the ferroelectric–paraelectric transition at $T_C = 420$ K.[8] A series of annealing steps were performed either under oxygen or a reductive atmosphere which led to disappearance of the space charge relaxation. Electric conductivity studies showed an extrinsic semiconduction of n-type behaviour. Comparison of activation energies showed the carriers to have a polaronic character, in good agreement with the low temperature existence of the relaxation.

An example of interface charge relaxations is $BaTiO_3$ ceramics doped by both niobium and cobalt.[9] For 0.9 mol% Nb and 0.3 mol% Co, a semiconducting behaviour was

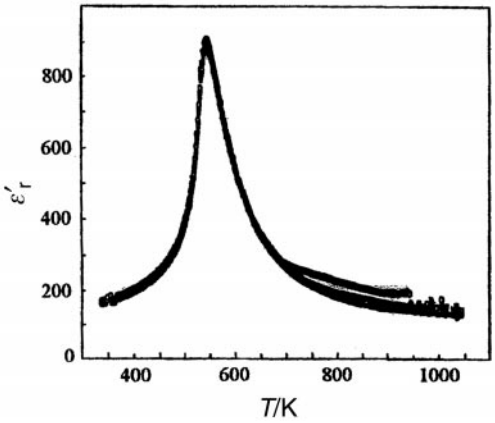

Fig. 5 Temperature dependence of ε'_r at three frequencies (10^4, 10^5 and 10^6 Hz) for a ceramic with composition $Ba_{0.7}Pb_{0.3}TiO_3$ sintered at low temperature.[5]

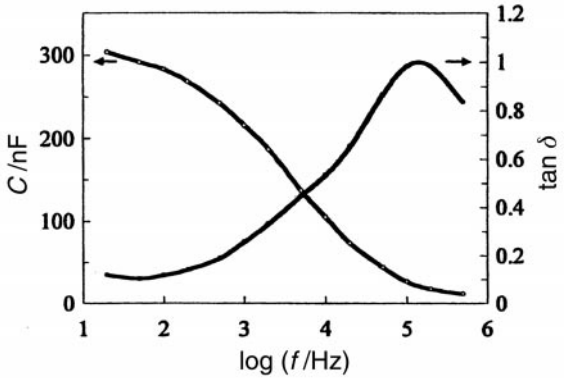

Fig. 6 Frequency dependences of C and tan δ for a ceramic of $BaTiO_3$ doped by both cobalt and niobium.[9]

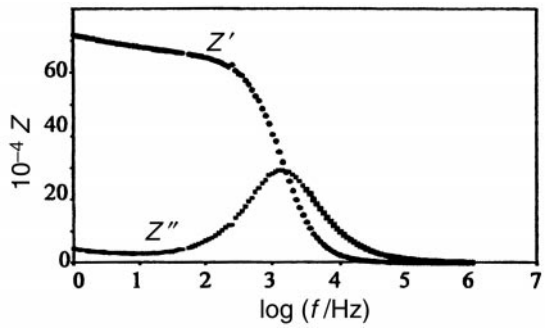

Fig. 7 Frequency dependences of Z' and Z'' for a ceramic with composition $Pb_{4.5}LiTa_{10}O_{30}$ at 600 K.

obtained. Strong apparent real dielectric constants due to Maxwell–Wagner polarisation were determined at 10^3 Hz. A dielectric relaxation also occurred around 10^5 Hz (Fig. 6). It was attributed to an interface charge relaxation at the grain boundaries, since a core shell structure was revealed by SEM studies.[10,11]

The two phenomena above were observed in a ceramic of composition $(K_{0.50}Na_{0.50})(Sr_{0.75}Ba_{0.25})_2Nb_5O_{15}$. One relaxation mechanism was explained in terms of a hopping process of space charge migration bound inside the ferroelectric grains, while the other was associated with interface charges at the grain boundary layers.[12]

Examination of frequency dispersion, whatever the structural type (perovskite or TKWB) and the temperature, implies that ε'_r is always decreasing from 10^2 to 10^6 Hz. In fact, such relaxations related to conductivity are more clearly observed in the same frequency range by studying the impedance variations, as stated in the definition section. The curves in Fig. 7 show very well the impedance relaxation rather than the dielectric one. Here the conductivity is ionic and due to Li^+ migration.[13,14]

For all space charge relaxations, the types and concentrations of charge carrier are correlated to defect chemistry and are affected by both temperature, oxygen partial pressure P_{O_2} during heat treatments, and the concentration of impurities or dopants. Annealing processes in the regime of conventionally oxidizing to moderately reducing atmospheres lead to a predominant ionic conductivity and some contribution of p-type electronic conductivity.[15,16] The mobile ionic species are either anions (O^{2-} and F^-) or cations (Li^+, Na^+,...) which move by a vacancy mechanism. Relations between conductivity, space charges, non-stoichiometry and defect chemistry have been studied in detail in acceptor-doped and donor-doped $BaTiO_3$.[11,17–19] Such effects are claimed to be at the origin of the PTCR mechanism.[20]

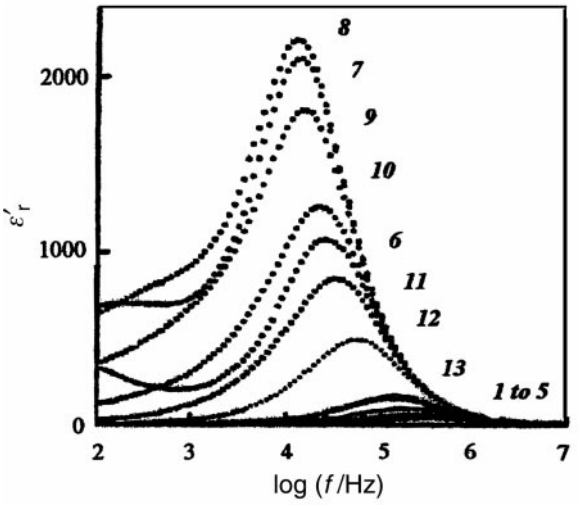

Fig. 8 Frequency variation of ε'_r for a ceramic with composition $KTa_{0.97}Nb_{0.03}O_3$ at various temperatures: 7.2 (1), 11.1 (2), 17.7 (3), 24.2 (4), 30.6 (5), 38.9 (6), 41.5 (7), 43.4 (8), 45.3 (9), 47.1 (10), 48.9 (11), 51.7 (12) and 60.9 K (13).[28]

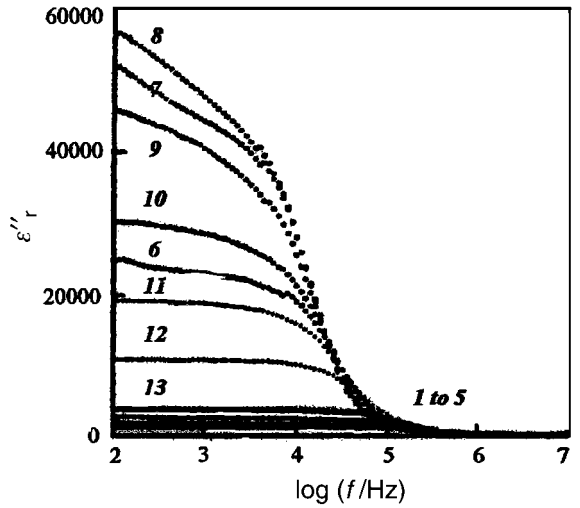

Fig. 9 Frequency variation of ε''_r for a ceramic with composition $KTa_{0.97}Nb_{0.03}O_3$ at various temperatures: 7.2 (1), 11.1 (2), 17.7 (3), 24.2 (4), 30.6 (5), 38.9 (6), 41.5 (7), 43.4 (8), 45.3 (9), 47.1 (10), 48.9 (11), 51.7 (12) and 60.9 K (13).[28]

Domain wall relaxations. In a domain structure (ceramic or single crystal), changes occurring under an electric field include both:

(1) The switching process of the polarization *i.e.* a P–E hysteresis loop (larger effect).

(2) Small oscillations of the domain walls which occur when measuring ε'_r under a small alternative electric field. At low frequency, dielectric relaxations appear (about 0.5–10^5 Hz). The relaxation frequency depends both on the thickness and the orientation (parallel for 180° domains, perpendicular for 90° domains) of the domain walls.

Near the Curie temperature, the distinction between the two effects tends to vanish. As the coercitive field is very weak, the low voltage leads to small oscillations which are large enough to induce the polarization switching process.

A model was advanced by Nettleton on wall inertia and the possible coupling of wall motion to dielectric relaxation.[21]

Moreover, studies were performed on ceramics or single crystals of $BaTiO_3$, KTN, PZT, PMN, $LiNbO_3$ and $Sr_2Nb_2O_7$.[22–27]

As an example, a very clear frequency dispersion was obtained with single crystals of $KTa_{1-x}Nb_xO_3$ ($x=0.03$).[28] Firstly, the authors showed, by various methods, that such materials exhibit the classical phase transition sequence:

$$\text{Rhomb.} \xrightarrow{T_1} \text{Orth.} \xrightarrow{T_2} \text{Tetrag.} \xrightarrow{T_c} \text{Cub.}$$

as in $KNbO_3$ and $BaTiO_3$. Figs. 8 and 9 show the dispersion of ε'_r and ε''_r *vs.* log(f) which is plotted for various temperatures from 7.2 to 60.9 K. A drastic step occurs at $f \sim 10^4$ Hz. The highest values of ε'_r lie between 38 and 49 K, *i.e.* close to $T_C \approx 42$ K. In fact, a polydispersive behaviour is observed for $T < 48.9$ K: when the frequency decreases, there is an additional increase in ε'_r to the strong decrease at $f \sim 10^4$ Hz. Such behaviour is corroborated by the Argand diagram $\varepsilon'_r = f(\varepsilon''_r)$: in the range $39 < T < 42$ K, there is an additional, well separated, extremely flat Cole–Cole semi-circle. Both relaxation effects decrease when T increases from T_C, in agreement with the disappearance of the ferroelectric properties, and of course, of the corresponding domains.

The domains, which are either ferroelectric or ferroelectric–ferroelastic, are induced by impurities, point defects and imperfections. These domains are created by mechanical stresses and tend to absorb the latter while developing along the crystallographic directions.

4.2. Medium-range frequency relaxation: the relaxors

Relaxors constitute a particular class of ferroelectric materials characterized by specific dielectric properties: a diffuse phase transition, an increase in the temperature of the maximum of permittivity, T_m, as the frequency increases and a dielectric relaxation in the range 10–10^7 Hz observed only in the ferroelectric phase (Figs. 10 and 11). The relaxor behaviour appears mainly in oxygen octahedron families *e.g.* in perovskite structure compositions, in tungsten bronze structure (TKWB) materials ($(A1)(A2)_2(C)_2(B1)(B2)_4O_{15}$ formula), *etc.* Among the perovskites, complex lead-based structures with two different cations in the same crystallographic site are particularly concerned. Well-known examples are $Pb(Mg_{1/3}Nb_{2/3})O_3$ [PMN] and $(Pb_{1-3x/2}La_x)(Zr_yTi_{1-y})O_3$ [PLZT].

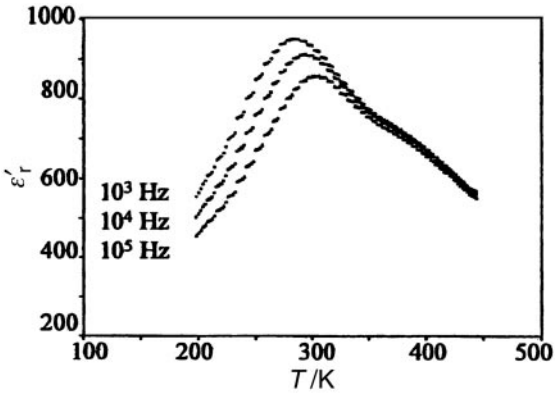

Fig. 10 Temperature dependence of ε'_r at various frequencies for a ceramic with composition $Pb_{4.1}K_{0.8}LiTa_{10}O_{30}$.

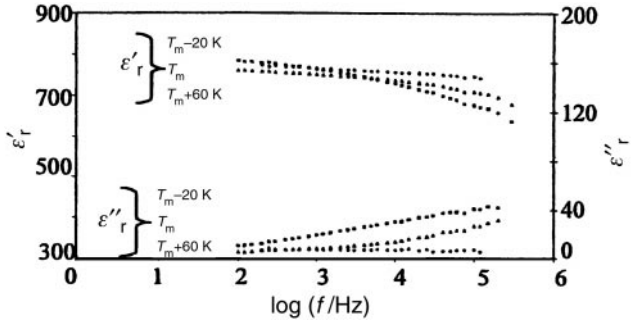

Fig. 11 Frequency dependences of ε'_r and ε''_r at various temperatures for a ceramic with composition $Pb_{4.1}K_{0.8}LiTa_{10}O_{30}$.

However, some lead-free compositions were also recently found to present relaxor properties *e.g.* ceramics with compositions derived from $BaTiO_3$ by homovalent or heterovalent substitutions ($BaTi_{1-x}Zr_xO_3$, $Ba_{1-x}Na_x(Ti_{1-x}Nb_x)O_3$,…). The compositions $Pb_{1-x}Ba_{1-x}Nb_2O_6$ and $Sr_{1-x}Ba_xNb_2O_6$ are two examples of TKWB type relaxors. A close relation exists between microstructural and/or nanostructural features and relaxor properties. There is an essential difference between the long-range and the short-range structures. The absence of a macroscopic symmetry change is specific to relaxor ferroelectric–paraelectric phase transitions. The strong low frequency relaxation observed in the dielectric response is characterized by a maximum of ε''_r as a function of frequency, which becomes broader with decreasing temperature from T_m. The associated fall in ε'_r extends over a very wide frequency range. Interactions between local polar moments prevent the use of a Debye model to describe the relaxation. A wide distribution of relaxation time is necessary. Such behaviour reflects the critical slowing down resulting from the increasing cooperative interactions between polar domains.

Various models have been proposed to explain the origin of the relaxor behaviour. An overview of the most significant models is briefly presented in order to underline the correlation between symmetry breaking defects and dispersive dielectric relaxation. In the first part which concerns lead-based perovskites, the discussion focusses essentially on the most well-known relaxor, PMN.

According to the superparaelectric model, a dielectric relaxation occurs due to thermally activated polarization reversals between equivalent variants.[29] This model describes the dynamics of the polar microregions in relation to temperature. The Vogel–Fülcher analysis is the basis of the dipole-glass model.[30] Freezing of the dipoles results from cooperative interactions between moments on the nanometer scale. The frequency dispersion of the real permittivity maximum can be described by the Vogel–Fülcher relation:

$$\omega = \omega'_0 \exp[-E_a/k(T_m - T_f)]$$

where ω is the frequency, E_a the activation energy and T_f the freezing temperature. As the temperature decreases, the relaxation is characterized by large relaxation time distributions. The system can be described as interactions of superparaelectric clusters with size dispersion leading to a glassy state. Near T_f, the long time relaxation reflects slow dynamics. The system is characterized by a break-up of a normal domain structure: a frozen polar state is reached at temperatures which are sufficiently low. Similarly, the random field model concerns the existence of domain states induced by fluctuations of quenched random fields arising from particular composition fluctuations.[31] A recent original model is based on a new atomic arrangement in the ordered Mg/Nb domains in PMN.[32] As a result of compositional disorder ($Nb/(Mg_{2/3}Nb_{1/3})$ alternate layer), lead atoms are locally displaced in random directions and the Pb local polarization is evaluated.

Theoretical models have been proposed in order to simulate the frequency dependence of the dielectric permittivity in relaxors. For example, a correlation between the low frequency dielectric behaviour and the size effect of polar domains (polar cluster volume distribution) has been evidenced.[33] A Monte-Carlo method was used to describe the frequency dispersion by considering the relaxor as an Ising-like dipole system.[34] The random field Potts model considers the effect of local fields resulting from a defect-centre (chemical domain walls).[35] Another interesting example is $Pb(Sc_{1/2}Ta_{1/2})O_3$ [PST]. Disordered PST resulting from quenching presents a diffuse phase transition and a relaxor behaviour. On the contrary, annealing increases the degree of order in the B cationic network and as a result, a classical ferroelectric behaviour is observed (sharp transition and no frequency dispersion). Here the important parameter regarding the relaxor effect is the cationic ordering, which influences the polar clusters.

The common point in the numerous studies on ferroelectric relaxors is the local distortion of the short-range structure, giving rise to local polar domains. These polar regions are closely related to order/disorder nanostructures, electric charge imbalance, local distortions due to ionic displacements, chemical textures, domain walls (random electric fields), *etc*… The resulting break in symmetry leads to a non long-range polar state, as is the case in classical ferroelectrics.

Concerning the lead-free ceramics derived from $BaTiO_3$, the relaxor effect is all the more favoured as the composition deviates from $BaTiO_3$ and as the substitution is heterovalent in the 6 C.N. crystallographic site. The relaxor phase has a local rhombohedral symmetry, after disappearance of the orthorhombic and tetragonal phases existing in $BaTiO_3$. These materials obey the Vogel–Fülcher law. Compared to those of $BaTiO_3$, their relaxor ferroelectric properties are due to compositional defects which may include non-stoichiometry. Such an effect was shown in insulator ceramics of composition $Ba_{1-x/2}\square_{x/2}(Ti_{1-x}Nb_x)O_3$, *i.e.* in the system $BaTiO_3$–$Ba_{0.5}NbO_3$.[36] In another way Nb-doping of $BaTiO_3$ was found *via* Ti-site vacancies, the material then being semiconductive.

In tungsten bronze type relaxor ferroelectrics, the complexity of the structure makes interpretations more difficult. Disorder usually takes place in the A1 (12 C.N.) and A2 (15 C.N.) sites. A very simple example concerns $BaNa_2Nb_{15}O_{14}F$ compared to $Ba_2NaNb_5O_{15}$. In the former, a relaxor ferroelectric, the A2 site is half-occupied by Ba^{2+} and Na^+, while in the latter, a classical ferroelectric, the A2 site is occupied only by Ba^{2+}.[37–40] Both lead-based and lead-free compositions have been found to be relaxors. Dielectric measurements performed on $Pb_2K(Nb_{0.1}Ta_{0.9})_5O_{15}$ showed a typical relaxor behaviour. Fig. 12 shows a relaxation with a broad relaxation time observed in the ferroelectric phase. This relaxation is interpreted by using a polar microdomain concept. Some

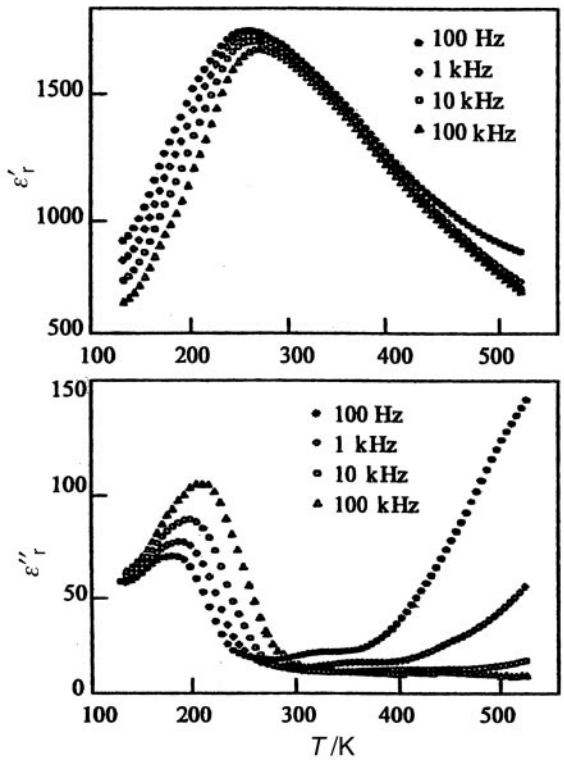

Fig. 12 Temperature dependences of ε'_r and ε''_r at various frequencies for a ceramic with composition $Pb_2K(Nb_{0.1}Ta_{0.9})_5O_{15}$.

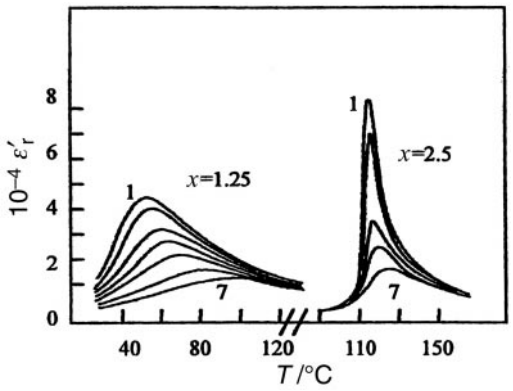

Fig. 13 Temperature dependence of the dielectric constant of a crystal with composition $Sr_{(5-x)}Ba_xNb_{10}O_{30}$ (SBN) at various frequencies from 1.5 Hz (1) to 7.2 MHz (7).[42]

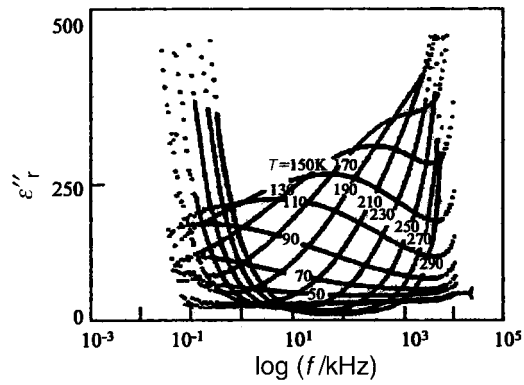

Fig. 15 Imaginary part of the dielectric constant of an *a*-axis $Pb_{0.65}Ba_{0.35}Nb_2O_6$ single crystal *versus* frequency at different temperatures.[45]

compositions belonging to the ternary diagram $Li_5Ta_5O_{15}$–$K_5Ta_5O_{15}$–$Pb_{2.5}Ta_5O_{15}$ also present relaxor properties. Thanks to structural, combinatorial calculations and dielectric studies, the influence of the cationic distribution in A sites was determined. Proof of relaxor behaviour in such TKWB families requires not only the presence of two different cations in the same crystallographic site (Pb, K) but also a critical proportion of cations Pb/Pb+K in the A2 site (A2 site at least half-occupied by lead atoms).[41] In $Sr_{1-x}Ba_xNb_2O_6$, the relaxation phenomena depend on the strontium content. The dispersion is more pronounced in Sr-rich compositions (Fig. 13). Compositional heterogeneity in solid solutions and structural disorder lead to a breakdown of translational symmetry. Local polarization fluctuations resulting from such local chemical inhomogeneity is thought to be at the origin of the relaxor nature of SBN.[42] The broad dielectric relaxation observed cannot be described by a single relaxation time (Fig. 14). Moreover, the wide distribution of relaxation times is temperature-dependent. The dielectric relaxation is observed when the thermal energy is of the order of magnitude of the potential barrier height of the local polarization state.[43] An anisotropic glassy behaviour was found in SBN for which the authors proposed a heterophase fluctuation model.[44]

Another example concerns the dielectric properties of morphotropic-phase-boundary lead barium niobate TKWB ($Pb_{1-x}Ba_xNb_2O_6$). A large dielectric relaxation phenomenon was evidenced (Fig. 15).[45] A thermally agitated local-polarization fluctuation model based on a superparaelectric relaxor concept was proposed. The influence of nanoscale chemical inhomogeneities in the Ba^{2+} and Pb^{2+} distribution on the perturbation of the polarization (magnitude and orientation) was suggested. Such perturbation is of a dynamic nature and explains the relaxation phenomena.

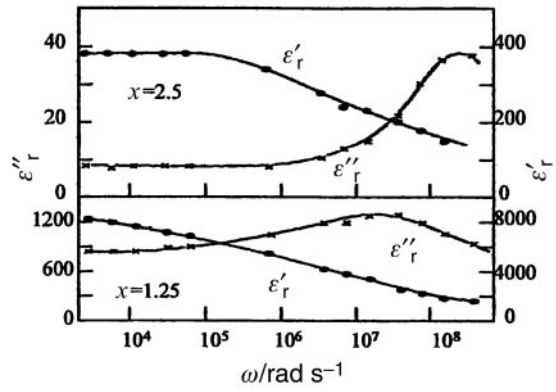

Fig. 14 Variations of ε'_r and ε''_r as a function of radian frequency ω at 296 K for a crystal with composition $Sr_{(5-x)}Ba_xNb_{10}O_{30}$ at 296 K.[42]

4.3. High frequency relaxations

The recent use of high, very high and ultra high frequencies in various domains—telecommunications, microelectronics, *etc.*—has triggered research on materials in this frequency range. The study of dielectric properties to evidence relaxations and to understand both the relaxation mechanisms and the modulation of physical properties is of prime importance for applications. From an experimental point of view, measurements in the frequency range between the highest dielectric frequencies ($f_r \sim 10^7$ Hz) and the lowest optical frequencies ($f \geqslant 10^{10}$ Hz) are becoming more and more important. Table 1 summarizes most of the recent data concerning relaxations in numerous displacive or order–disorder ferroelectrics: perovskites, tetragonal tungsten bronzes, *etc.*[46–58] Such high frequency relaxations have been ascribed to different origins. A description of the suggested models is given. Of course such a list is not exhaustive but refers to the main mechanisms proposed to date.

Relaxation was first attributed to the piezoelectric resonance of the domains resulting from piezoelectric deformations of the polarized domains in an alternating electric field.[59]

Strong dielectric dispersion was observed in barium titanate. The origin was attributed to the resonance of the grains and is thus closely related to the microstructure.[60]

The dielectric response of lithium niobate was then studied on ceramics. $LiNbO_3$ possesses only 180° domains; the relaxation step observed was thus explained by piezoelectric sound emission from the crystalline grains of the ceramics.[61]

In a polydomain single crystal, the dielectric response between 10^6 and 10^8 Hz was suggested to be dominated by the piezoelectric resonance of the individual domains.[62]

Relaxation between 30 MHz and 3 GHz was also ascribed to

Table 1 Relaxation frequency for various ferroelectric materials

Sample	Relaxation frequency (f_r/Hz)	Ref.
$KTaO_3$ crystal	5×10^7 (4 K)	46
$BaTiO_3$ crystal	2×10^8 (410 K)	47
$BaTiO_3$ ceramic	2×10^8 (410 K)	48
$BaTiO_3$: Ca, Pb, Zr ceramics	$1 \times 10^8 < f_r < 1 \times 10^9$ (300 K)	48
PZT ceramics	5×10^8 (300 K)	49
PMN ceramics	4×10^7 (267 K)	50
PMN-PT ceramics	2.1×10^7 (339 K)	50
PIN ceramics	1.3×10^8 (347 K)	50
PZT thin films	10^7 (300 K)	51
PZT ceramics	$3 \times 10^8 < f_r < 1 \times 10^9$ (300 K)	52
$K_{0.86}Li_{0.14}TaO_3$ crystal	1×10^9 (135 K)	53
RbD_2PO_4 crystal	1×10^9 (329 K)	54
$Ba_2NaNb_{2.15}Ta_{2.85}O_{15}$ crystal	3×10^8 (396 K)	55
$Sr_{0.3}Ba_{0.7}Nb_2O_6$ ceramic	3×10^8 (365 K)	56
$Pb_{3.75}K_{1.5}LiTa_{10}O_{30}$ ceramic	3.5×10^8 (240 K)	57
PST ceramic	5.5×10^8 (245 K)	58

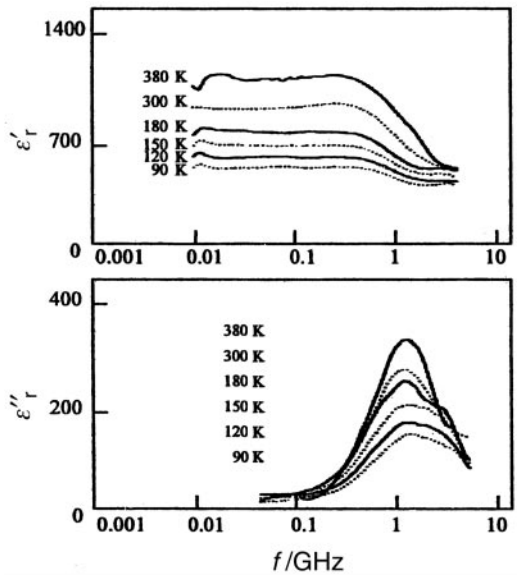

Fig. 16 Temperature dependences of the relaxation curves of a tetragonal lead zirconate titanate ceramic.[63]

the ferroelastic domain walls. Displacement of the ferroelastic 90° domain walls leads to a deformation of the material. In a.c. fields, vibrational displacements of the walls create elastic waves and the domain wall is considered to behave as a shear wave transducer. Relaxation has been shown to approximate a Debye relaxation. In perovskite-type ferroelectrics, the domain width is of the order of 1 μm, so relaxation should appear between 0.5 and 1 GHz (Fig. 16).[63] An additional cause for dielectric dispersion has been suggested: piezoelectric sound generation by domains. In both single crystals and ceramics, the deformation of laminar domains under an electric a.c. field is excited by the piezoelectric effect. The resulting sound emission causes a dielectric relaxation. Such a dispersion can appear even in ferroelectrics which have no ferroelastic domain walls.[64]

Another model based on the effect of the hopping of off-centred ferroelectric ions has also been proposed by several authors.[47–65] The relaxation observed in perovskite-type ferroelectrics is in the range 10^7–10^9 Hz. According to the structural investigations of Comes *et al.*,[66] the relaxing dipoles can be ascribed to chains of active ferroelectric ions (Ti^{4+} in $BaTiO_3$; Nb^{5+} in $Pb(Mg_{1/3}Nb_{2/3})O_3$;...) which are displaced from the centre of the oxygen octahedra. A correlated relaxation of these chains is believed to induce a macroscopic radio-frequency dispersion. Measurements performed without discontinuities between 10^2 and 10^{14} Hz showed a strong relaxation, close to 10^8 Hz, in $Pb(Sc_{1/2}Ta_{1/2})O_3$.[58]

High frequency studies on ceramics or crystals of tetragonal tungsten bronze structure (TKWB) also evidenced a dipolar

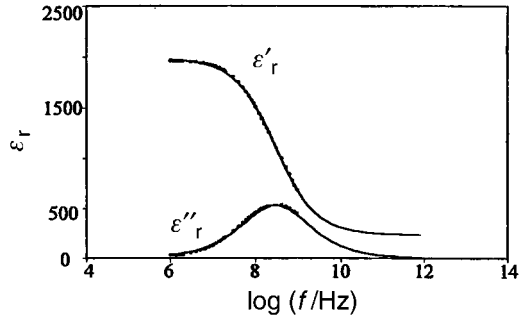

Fig. 17 Frequency dependences of ε'_r and ε''_r at 365 K for a ceramic with composition $Sr_{0.3}Ba_{0.7}Nb_2O_6$ (● experimental points, — theoretical curves).

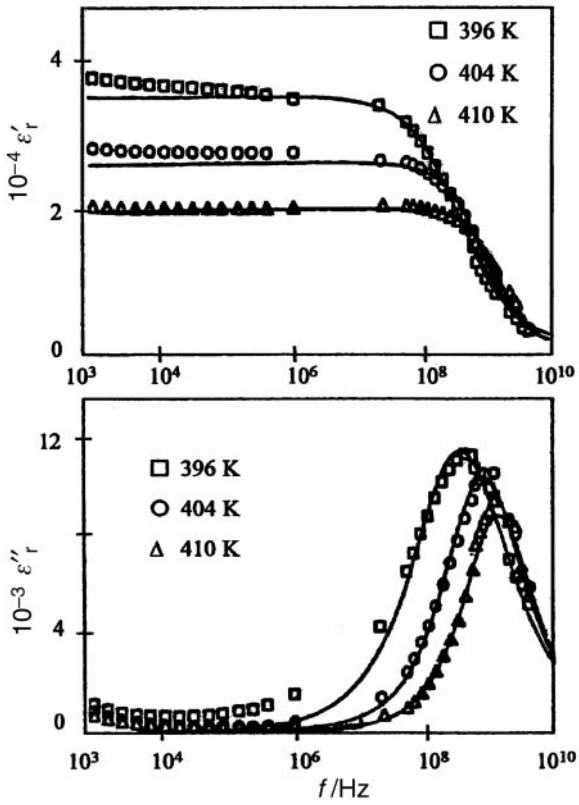

Fig. 18 Frequency dependences of ε'_r and ε''_r at various temperatures in the paraelectric phase of a ceramic with composition $Ba_2NaNb_{5(1-x)}$-$Ta_{5x}O_{15}$ (● experimental points, — theoretical curves).[55]

relaxation in the range 10^8–10^9 Hz. Strontium barium niobate, $Sr_{0.3}Ba_{0.7}Nb_2O_6$, exhibits a high frequency (HF) relaxation in the paraelectric phase and its origin was ascribed to the crystalline network owing to the motion of active ferroelectric Nb^{5+} ions (Fig. 17).[56] HF relaxation was also observed in ceramics of the $K_3Li_2Ta_5O_{15}$–$Pb_{2.5}Ta_5O_{15}$ system. A microscopic origin of this relaxation in relation with cooperative hopping of Ta^{5+} along the correlation chains was proposed.[57] Another example concerns the investigation of a TKWB crystal ($Ba_2NaNb_{5(1-x)}Ta_{5x}O_{15}$); a relaxation was found close to 10^8 Hz (Fig. 18). The relaxational mode is thought to be related to the unharmonic motion of Nb(Ta) atoms in a double-well potential in NbO_6 octahedra.[55]

A last example concerns the dielectric study of $K_{0.86}Li_{0.14}TaO_3$ in the frequency range 10^3–10^{10} Hz.[67] Here an ionic mechanism was proposed. The relaxation is thought to be caused by thermally activated motions of separate Li^+ ions in the multi-minima lattice potential. The interactions between Li^+ are very weak, in agreement with Debye-type relaxation (no spectral distribution, Cole–Cole parameter $\alpha < 0.1$).

With reference to the above models, the following discussion will underline the link between high frequency relaxation and considerations such as microstructure, defects, and chemical bonds. As seen above, several models involve mechanisms based on the piezoelectric resonance of grains, domains and sound emission from ferroelastic domain walls. Naturally, these models are closely related to the microstructure. As a result, numerous studies have concerned the high frequency dielectric properties of ferroelectric ceramics in relation to grain size. For example, in $BaTiO_3$ ceramics and $BaTiO_3$ powder–polymer matrix composites, relaxation or resonance (grain size 0.26 μm, particle size 66 nm) were evidenced. The relaxation frequency was found to increase with decreasing grain/particle size. The role of the domain width in the control of the relaxation frequencies was suggested.[68] The strong dependence of relaxation frequency on grain size in coarse and

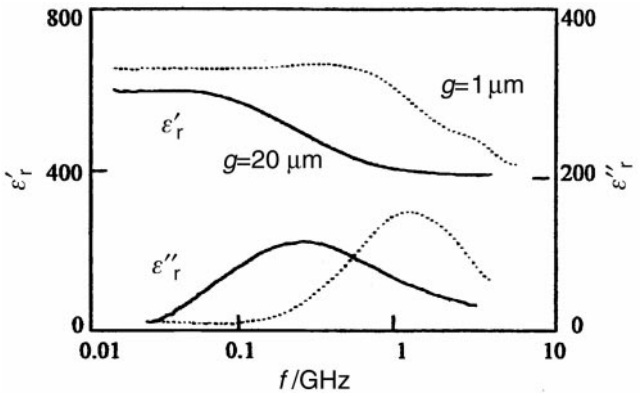

Fig. 19 Dielectric dispersion in coarse or fine grained lead zirconate titanate $PbZr_{0.52}Ti_{0.48}O_3$ ceramic.[69]

fine grained lead zirconate titanate (PZT) has also been shown (Fig. 19). Defects have also been considered because of their influence on domain wall mobility.[69] Note that in various studies, high frequency measurements were performed at different temperatures on both $BaTiO_3$ ceramics and crystals; different values of ε'_r and ε''_r, but very similar relaxation frequency values were obtained (Fig. 20).[47,48,70] Moreover, in order to study the influence of piezoelectric domain resonance on dielectric dispersion, dielectric measurements were performed *versus* temperature on both poled and unpoled samples. Piezoelectric resonance in the range 10^6–10^7 Hz appeared on the poled sample. Such a resonance coexists with a Cole–Cole relaxation ($f_r \sim 7 \times 10^8$ Hz) in the ferroelectric region; on the contrary, it was shown that only dielectric relaxation remains above the Curie temperature.[65]

The temperature dependence of high frequency relaxation is still a matter of controversy. Many investigations have concluded that the relaxation frequency is almost independent of temperature up to T_C.[63] On the contrary, relaxation frequencies were reported elsewhere to decrease critically at the Curie temperature.[68–71] A minimum of f_r (HF) at T_C was also found in various types of material such as lead-based complex perovskites (PMN, PMN-PT)[50,72] (Fig. 21) and materials without octahedra such as triglycine sulfate,[73] $NaNO_2$[74] and RbD_2PO_4.[54] On the contrary, in TKWB ferroelectrics, the temperature variation of the relaxation frequency is smooth in the vicinity of the Curie temperature.[55,56,75]

The effect of ionic substitutions on f_r values has been widely studied. In the correlation chain model, the substitution effect is related to an octahedron distortion and thus to a change in the displacement of the ferroelectric ions. The change in f_r values is correlated with a modification of the chain length.[48] In PZT, an increase in relaxation frequency with increasing Ti

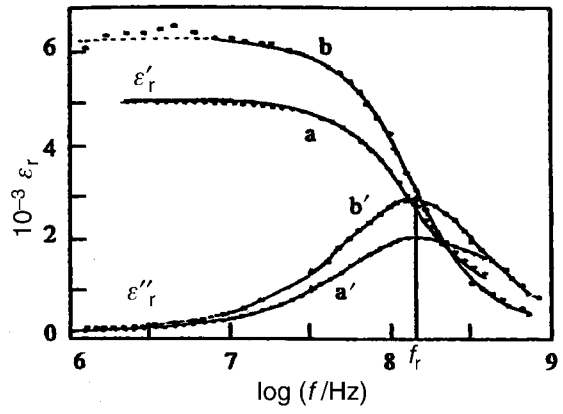

Fig. 20 Frequency variations of ε'_r and ε''_r for $BaTiO_3$ ceramic (a, a′) or crystal (b, b′).

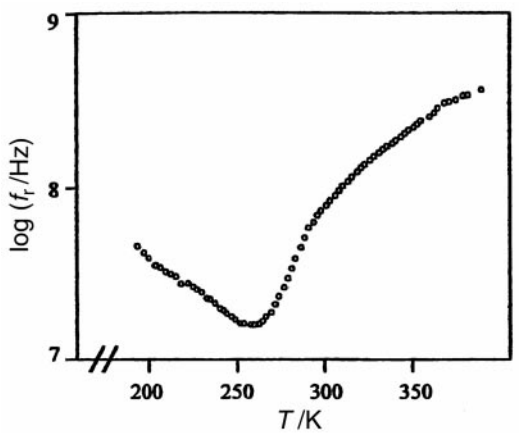

Fig. 21 Temperature dependence of the relaxation frequency for a ceramic with composition $Pb(Mg_{1/3}Nb_{2/3})O_3$.

content was observed.[52] The Extended Hückel Tight-Binding method [EHTB] was used as a theoretical tool in the comparative study of $Pb(Sc_{1/2}Nb_{1/2})O_3$ [PSN] and $Pb(In_{1/2}Nb_{1/2})O_3$ [PIN]. Differences between the PIN and PSN density of state curves are mainly due to indium and scandium. Concerning Nb–O and Sc–O, the same type of orbital interaction is involved, whereas In–O and Nb–O bonds exhibit large differences both in symmetry and ionicity. As a result Sc^{3+} ions are believed to be involved in the correlation chain with Nb^{5+}. On the contrary, indium probably breaks the chains leading to a lower value of f_r in PIN compared to the PSN f_r value.[76] In $K(Ta_{1-x}Nb_x)O_3$ (KTN), an increase in covalency with Ta content was shown to stiffen the metal–oxygen network enough to change the relaxational dynamics and lead to a shift of f_r values.[77,78]

High frequency relaxation exists in materials of various chemical composition and structure. The existence of the relaxation in both perovskite and TKWB type ferrolectrics accounts for a phenomenon closely related to oxygen octahedra. The systematically higher f_r (HF) values in TKWB compared to perovskite materials are due to the mono-dimensionality and the strong anisotropy of the TKWB structure.[75]

Finally, although the existence of a dielectric relaxation in the range 10^7–10^{10} Hz is well established, its origin is still a matter of debate. Moreover, the contribution of cationic or anionic vacancies, unwanted defects and impurities has not yet been really quantified.

4.4. Dielectric response above the microwave region

This short section will deal with the study of ferroelectric materials above the microwave frequency range. Even if this does not directly concern relaxation phenomena, the importance of such experiments both for the study of phase transition mechanisms and to be able to predict the dispersion at lower frequency (relaxational character), justify a brief discussion within the scope of this article.

The microwave frequency range can be divided into three wave bands: the centimeter wave band (3 to 30 GHz) (also commonly called the microwave region), the millimeter wave band (30 to 300 GHz) and the submillimeter wave band (300 to 3000 GHz). The phonon contribution governs the complex permittivity in the dielectric response above 100 GHz. This response has a resonant character in soft mode systems (Raman spectroscopy). When the response has a relaxational character, the dispersion lies in the centimeter wave band or radio-frequency range. A soft mode frequency of various ferroelectrics comes into the microwave range close to the Curie temperature. In addition, central peak type excitations may be evidenced in Raman spectra close to the phase

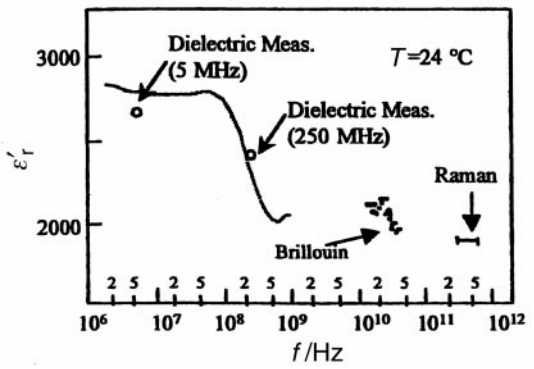

Fig. 22 Quantitative agreement between several data from different experiments dealing with the dynamical spectrum of $BaTiO_3$.[83]

transitions. Even if the occurrence of a central peak does not systematically imply a relaxation, some models take into account the coupling between the soft mode and possible relaxors. Models may also involve coupling of the soft mode to the localized impurity mode (disorder), giving rise to a dielectric dispersion in the microwave or lower frequency ranges.[79] When a lattice mode softens, a part of the dynamic response may fall into the range 10^9–10^{10} Hz. On approaching T_C, the soft mode becomes overdamped. As a result, an anharmonic motion in a local potential can appear (relaxation) and a crossover from displacive to order–disorder behaviour occurs.[80] The following examples illustrate such a contribution of the relaxational type in the GHz or sub-GHz ranges.

In $BaTiO_3$, infrared absorption experiments demonstrated the crossover from displacive to order–disorder of the phase transition. A relaxation component was included in the dielectric spectrum at frequencies lower than the soft mode frequencies. EPR, NMR experiments and analysis of the central peak in Raman spectra confirmed that the relaxation frequency should lie at a frequency 10^{10} Hz lower (Fig. 22).[81–83] For temperatures close to T_C, it seems that there is a splitting into the overdamped soft mode and a relaxation frequency which slows down to 2×10^8 Hz.[84]

First order Raman scattering in KTN and KLT revealed a phonon softening; a minimum value of 1 cm^{-1} ($\sim 5 \times 10^{10}$ Hz) was reached close to 20 K in KTN. Polar microregions are believed to be induced by randomly distributed, interacting off-center ions in highly polarizable host crystals such as $KTaO_3$.[85] An intense central peak was evidenced in the Raman spectra.[86]

Several disordered ferroelectrics have been described with infrared and microwave spectroscopies. Overdamped modes appear below the polar mode range (centimeter to submillimeter ranges). These modes are connected with strongly anharmonic vibrations of some of the ions of nanosized polar clusters.[87]

A final example is the report of the submillimeter dielectric response of a PLZT 9.5/65/35 relaxor thin film. Near room temperature, the structure was described as a dense system of uncorrelated dynamic polar clusters. A pronounced broad dispersion was found below the soft mode response in the 10^{10}–10^{12} Hz range. The origin was attributed to volume fluctuations of the polar nanoclusters (vibration of the charged intercluster boundaries); flipping into different orientations of these polar clusters was connected with the lower frequency dispersion in the 10^5–10^8 Hz range.[88] Such wide band dielectric spectroscopy has made it possible to identify two different dispersion regions. Recent work has concerned microwave and infrared studies on relaxor ferroelectric ceramics PLZT 8/65/35 and 9.5/65/35. The infrared spectra gave evidence of the existence of polar nanoclusters. A softening of the lowest polar mode was observed close to the temperature where the clusters appeared. Below this temperature an additional strong microwave dispersion appeared in the frequency range

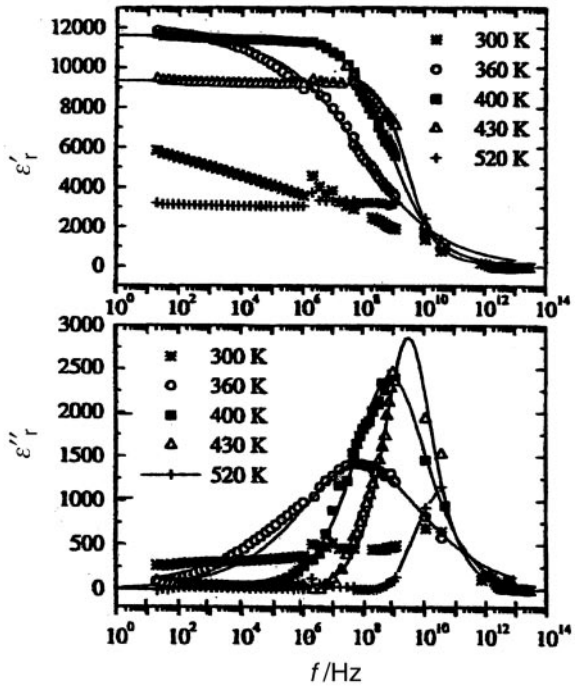

Fig. 23 Frequency dependences of ε'_r and ε''_r of a PLZT8/65/35 ceramic at various temperatures (● experimental points, — theoretical curves).[89]

10^7–10^{11} Hz.[89] Fig. 23 represents the frequency dependence of real and imaginary parts of the complex permittivity of PLZT 8/65/35 at various temperatures. The values above 10^{12} Hz are taken from the fit of room temperature infrared spectra.

Local spectroscopies such as infrared and Raman are thus of particular interest in the investigation of local dynamic disorder. Information on the nanometer scale, which is useful in systems such as complex perovskites, has now been obtained. In this way, the influence of impurities, composition, and ionic ordering have been widely studied.[90–92]

5. Conclusion

The various types of dielectric relaxations in octahedral-type ferroelectrics have been presented. Links between the value of the relaxation frequency, f_r, and the scale of the defect have been pointed out:

(1) Space charge relaxations ($\sim 10^2$–10^6 Hz) are related to conductivity phenomena. Here the f_r value is governed by defect chemistry (charge carriers) which depends on synthesis conditions (temperature, partial oxygen pressure, *etc.*).

(2) Domain wall relaxations ($\sim 10^2$–10^6 Hz) are closely connected to impurities and point defects.

(3) In relaxor ferroelectrics ($\sim 10^3$–10^6 Hz), the role of the nanostructure has been underlined.

(4) High frequency relaxation ($\sim 10^7$–10^{10} Hz) is correlated either to piezoelectric resonance of domains, or to a correlation chain model.

The more the "defect" is spatially localized, the higher the relaxation frequency is. The relaxation frequency thus appears to be inversely proportional to the scale of the phenomenon at the origin of the relaxation. Therefore, chemists can act on the microstructure (heat treatment), the nanostructure (order–disorder), or chemical bonding (composition), on one hand, to induce a type of relaxation and on the other hand, to tune the corresponding relaxation frequency. Such a predictive aspect could be a precious tool in the field of research into new materials for applications.

References

1 K. S. Cole and R. H. Cole, *J. Chem. Phys.*, 1951, **19**, 1484.
2 A. K. Jonscher, *J. Phys. D: Appl Phys.*, 1999, **32**, R57.
3 R. Coelho and B. Aladenize, *Les Diélectriques*, Hermès, Paris, 1993.
4 P. Goux, Thesis, University of Bourgogne, 1994.
5 O. Bidault, P. Goux, M. Kehikech, M. Belkaoumi and M. Maglione, *Phys. Rev. B*, 1994, **49**, 7868.
6 V. Andriamanpianina, J. Ravez, M. Dong and J. M. Réau, *C. R. Acad. Sci. IIb*, 1995, **321**, 467.
7 M. Dong, Thesis, University of Bordeaux, 1997.
8 A. Abalhassain, J. Ravez, J. P. Doumerc and M. Elaatmani, *J. Phys. III*, 1996, **6**, 863.
9 D. Lavielle, J. Poumarat, Y. Montardi, P. Bernard and O. Aguerre-Chariot, *Proc. Eur. Ceram. Soc.*, 1991, 1903.
10 M. Belkaoumi, M. Maglione and B. Jannot, *Ferroelectrics*, 1990, **108**, 141.
11 D. Hennings and G. Rosenstein, *J. Am. Ceram. Soc.*, 1984, **67**, 249.
12 S. Bu, E. Shin and G. Park, *Appl. Phys. Lett.*, 1998, **73**, 1442.
13 V. Hornebecq, J. M. Réau and J. Ravez, *Solid State Ionics*, 2000, **127**, 231.
14 V. Hornebecq, personal communication.
15 D. M. Smyth, *Ferroelectrics*, 1994, **151**, 115.
16 R. Waser, *Ferroelectrics*, 1994, **151**, 125.
17 G. H. Jonker, *Solid State Electron.*, 1964, **7**, 895.
18 N. H. Chan, R. K. Sharma and D. M. Smyth, *J. Am. Ceram. Soc.*, 1982, **65**, 167.
19 N. H. Chan and D. M. Smyth, *J. Am. Ceram. Soc.*, 1984, **67**, 285.
20 W. Heywang, *J. Mater. Sci.*, 1971, **6**, 1214.
21 R. E. Nettleton, *J. Phys. Soc. Jpn.*, 1967, **6**, 1214.
22 V. V. Daniel, *Dielectric relaxation*, Academic Press, London, 1967.
23 L. Benguigui, *Ferroelectrics*, 1974, **7**, 315.
24 B. N. Prasolov, *Bull. Russ. Acad. Sci.*, 1993, **57**, 1003.
25 R. Herblet, U. Robels, H. Dederichs and G. Arlt, *Ferroelectrics*, 1989, **98**, 107.
26 V. P. Bovtun, N. N. Krainik, L. A. Markova, Yu. M. Poplavko and G. A. Smolenski, *Sov. Phys. Solid State*, 1984, **26**, 225.
27 A. V. Shilnikov, N. M. Galiyarova, S. V. Gorin, E. G. Nadolinskaya, D. G. Vasiliev and L. N. Vologuirova, *Ferroelectrics*, 1989, **98**, 3.
28 D. Sommer, D. Friese, W. Kleemann and D. Rytz, *Ferroelectrics*, 1991, **124**, 231.
29 L. E. Cross, *Ferroelectrics*, 1987, **76**, 241.
30 D. Viehland, M. Wuttig and L. E. Cross, *Ferroelectrics*, 1991, **120**, 71.
31 V. Westphal, W. Kleemann and M. D. Glinchuck, *Phys. Rev. Lett.*, 1992, **68**, 847.
32 T. Egami, *Ferroelectrics*, 1999, **222**, 163.
33 Z. G. Lu and G. Calvarin, *Phys. Rev. B*, 1995, **51**, 2694.
34 H. Gui, B. Gu and X. Zhang, *J. Appl. Phys.*, 1995, **78**, 1934.
35 H. Qian and L. A. Bursill, *Int. J. Mod. Phys. B*, 1996, **10**, 2007.
36 J. Ravez and A. Simon, *J. Korean Phys. Soc.*, 1998, **32**, 955.
37 R. Von der Mühll and J. Ravez, *Bull. Soc. Fr. Mineral. Cristallogr.*, 1975, **98**, 118.
38 J. P. Jamieson, S. C. Abrahams and J. L. Bernstein, *J. Chem. Phys.*, 1969, **50**, 4352.
39 P. Labbe, H. Leligny, B. Raveau, J. Schneck and J. C. Toledano, *J. Phys. Cond. Matter*, 1990, **2**, 25.
40 J. Ravez, H. El Alaoui-Belghiti and A. Simon, *Mater. Lett.*, 2001, **47**, 159.
41 V. Hornebecq, C. Elissalde, F. Weill, A. Villesuzanne, M. Menetrier and J. Ravez, *J. Appl. Crystallogr.*, 2000, **33**, 1037.
42 A. M. Glass, *J. Appl. Phys.*, 1969, **40**, 12.
43 J. M. Povoa, R. Guo and A. S. Bhalla, *Ferroelectrics*, 1994, **158**, 283.
44 D. Viehland and W.-H. Huang, *Ferroelectrics*, 1994, **158**, 301.
45 R. Guo, A. S. Bhalla, C. A. Randall and L. E. Cross, *J. Appl. Phys.*, 1990, **67**, 6405.
46 M. Maglione, U. T. Hochli and S. Rod, *Europhys. Lett.*, 1987, **4**, 631.
47 M. Maglione, R. Böhmer, A. Loidl and U. T. Hochli, *Phys. Rev. B*, 1989, **40**, 11441.
48 S. Kazaoui, J. Ravez, C. Elissalde and M. Maglione, *Ferroelectrics*, 1992, **135**, 85.
49 S. Li, J. Sheen, J. Jang, A. S. Bhalla and L. E. Cross, *Ferroelectr. Lett.*, 1993, **16**, 21.
50 C. Elissalde, Thesis, University of Bordeaux, 1994.
51 M. Sayer, A. Mansingh, A. K. Arora and A. Lo, *Integr. Ferroelectr.*, 1992, **1**, 129.
52 U. Böttger and G. Arlt, *Ferroelectrics*, 1992, **127**, 1431.
53 M. A. Leschenko, Yu. M. Poplavko and V. P. Bovtun, *Ferroelectrics*, 1992, **131**, 213.
54 R. R. Levitsky, I. R. Zachek, I. V. Kutny, J. J. Shur, J. Grigas and R. Mizeris, *Ferroelectrics*, 1990, **110**, 85.
55 R. Mizaras, M. Takashige, J. Banys, S. Kojima, J. Grigas, S. I. Hamazaki and A. Brilingas, *J. Phys. Soc. Jpn.*, 1997, **66**, 2881.
56 C. Elissalde and J. Ravez, *J. Mater. Chem.*, 2000, **10**, 681.
57 V. Hornebecq, C. Elissalde, J. M. Réau and J. Ravez, *Phys. Status Solidi A*, 1998, **169**, 311.
58 V. Bovtun, V. Porokhonskyy, J. Endal, J. Petzelt and C. Elissalde, *Ferroelectrics*, 2000, **238**, 17.
59 A. F. Devonshire, *Philos. Mag.*, 1951, **42**, 1065.
60 A. Von Hippel, *Z. Phys.*, 1952, **133**, 158.
61 Y. Xi, H. McKinstry and L. E. Cross, *J. Am. Ceram. Soc*, 1983, **66**, 637.
62 A. V. Turik and G. I. Khasabova, *Ferroelectrics*, 1978, **18**, 91.
63 G. Arlt, U. Böttger and S. Witte, *Ann. Phys.*, 1994, **3**, 578.
64 G. Arlt, U. Böttger and S. Witte, *J. Am. Ceram. Soc.*, 1994, **78**, 1097.
65 S. Kazaoui, Thesis, University of Bordeaux, 1991.
66 R. Comes, M. Lambert and A. Guinier, *Solid State Commun.*, 1968, **6**, 715.
67 M. A. Leschenko, Yu. M. Poplavko and V. P. Bovtun, *Ferroelectrics*, 1992, **131**, 213.
68 M. P. McNeal, S. J. Jang and R. E. Newnham, *J. Appl. Phys.*, 1998, **83**, 3288.
69 G. Arlt, *Electroceramics IV*, Verlag, Aachen, Germany, 1994, vol. 1, p. 193.
70 A. V. Turik and N. B. Schevchenko, *Phys. Status Solidi B*, 1979, **95**, 585.
71 U. Böttger, Thesis, RWTH Aachen, 1994.
72 V. Bovtun, M. A. Leschenko and Yu. I. Yakimenko, communication at *Matériaux et composants Piézo-Pyro-Ferroélectriques*, Limoges, 1996.
73 T. S. Benedict and J. L. Durand, *Phys. Rev. B*, 1958, **109**, 1091.
74 I. Hatta, *J. Phys. Soc. Jpn.*, 1968, **24**, 1043.
75 V. Hornebecq, Thesis, University of Bordeaux, 2000.
76 C. Elissalde, A. Villesuzanne, J. Ravez and M. Pouchard, *Ferroelectrics*, 1997, **199**, 131.
77 A. Villesuzanne, C. Elissalde, M. Pouchard and J. Ravez, *Eur. Phys. J.*, 1998, **B6**, 307.
78 C. Elissalde, A. Villesuzanne, V. Hornebecq and J. Ravez, *Ferroelectrics*, 1999, **229**, 1.
79 J. Grigas, *Microwave Dielectric Spectroscopy of Ferroelectrics and Related Materials*, Gordon and Breach, Amsterdam, 1996.
80 F. Gervais, *Ferroelectrics*, 1984, **53**, 91.
81 K. A. Müller, W. Berlinguer, K. W. Blazey and J. Albers, *Solid State Commun.*, 1988, **61**, 21.
82 A. Hackmann, O. Kanert, H. Kolen, H. Schultz, K. A. Müller and J. Albers, *Proceedings of ICDIM*, 1988.
83 K. Laabidi, M. Fontana, M. Maglione, B. Jannot and K. A. Müller, *Europhys. Lett.*, 1994, **26**, 309.
84 M. Maglione, *Ferroelectrics*, 1992, **137**, 113.
85 P. Di Antonio, R. E. Vugmeister, J. Toulouse and L. A. Boatner, *Phys. Rev. B*, 1993, **47**, 10.
86 P. Di Antonio, J. Toulouse, B. E. Vugmeister and S. Pilzer, *Ferroelectr. Lett.*, 1994, **17**, 115.
87 J. Petzelt, *J. Korean Phys. Soc.*, 1998, **32**, S482.
88 I. Fedorov, J. Petzelt, V. Železný, A. A. Volkov, M. Kosec and V. Delalut, *J. Phys. Cond. Matter*, 1997, **9**, 5205.
89 S. Kamba, V. Bovtun, J. Petzelt, I. Rychetsky, R. Mizaras, A. Brilingas, J. Banys, J. Grigas and M. Kosec, *J. Phys. Cond. Matter*, 2000, **12**, 497.
90 I. G. Siny, R. Tao, R. S. Katiyar, R. Guo and A. S. Bhalla, *J. Phys. Chem. Solids*, 1998, **59**, 181.
91 J. Petzelt, S. Kamba and I. Gregora, *Phase Transitions*, 1997, **63**, 107.
92 L. A. Bássora and J. A. Eiras, *Ferroelectrics*, 1999, **223**, 285.